Desalination and Water Treatment
www.deswater.com

doi: 10.5004/dwt.2020.24802

177 (2020) 330–337
February

Exploring the potential of Landsat-8 OLI and Sentinel-2 MSI data for mapping and monitoring Enez Dalyan Lagoon

Gizem Senel[a], Ahmet Ozgur Dogru[b], Cigdem Goksel[b,*]

[a]*Department of Geomatics Engineering, Graduate School of Science Engineering and Technology, Istanbul Technical University, 34469 Maslak, Istanbul, Turkey, Tel. +90 537 437 6379; email: senelgi@itu.edu.tr*
[b]*Department of Geomatics Engineering, Faculty of Civil Engineering, Istanbul Technical University, 34469 Maslak, Istanbul, Turkey, Tel. +90 212 285 6913; email: goksel@itu.edu.tr (C. Goksel), Tel. +90 212 285 3806; email: ozgur.dogru@itu.edu.tr (A.O. Dogru)*

Received 12 July 2019; Accepted 21 August 2019

ABSTRACT

This study investigated the coastal lagoon monitoring and mapping potential of Landsat-8 Operational Land Imager (OLI) and Sentinel-2 Multi-Spectral Instrument (MSI) in the Enez Dalyan Lagoon, located in Turkey. Five different water indices, including normalized difference water index (NDWI), modified normalized difference water index (MNDWI), automated water extraction index for shadow ($AWEI_{sh}$) and non-shadow ($AWEI_{nsh}$), tasseled cap wetness index (TCWI), and maximum likelihood classification methods were compared to evaluate the potential for mapping coastal lagoons. Additionally, spectral consistency of index algorithms was examined to introduce the coastal lagoon monitoring potential whereas cross-calibration analysis was carried out. Among the methods, the $AWEI_{nsh}$ achieved quite better results compared with the other methods for mapping Enez Dalyan Lagoon while TCWI had relatively poor results independent from the sensors. $AWEI_{nsh}$ had the strongest correlation with 0.989, while NDWI had the poorest correlation value as 0.966. Results pointed out the linear correlation and spectral consistency between almost all corresponding indices derived from the data of two sensors. This research indicated that index algorithms provide a reliable mapping of Enez Dalyan Lagoon. Also, Landsat-8 OLI and Sentinel-2 MSI sensors, which are statistically consistent, provided sufficient monitoring of Enez Dalyan Lagoon to both continuity and combined use.

Keywords: Coastal lagoon monitoring; Landsat-8; Sentinel-2; Spectral water index algorithms; Normalized difference water index

1. Introduction

Coastal lagoons are an integral part of aquatic ecosystems that are commonly shallow, marine-influenced water bodies [1,2]. The geomorphological development stages of the lagoons are in the form of swamps and then the complete land due to the changing ecological environment conditions. They are isolated from the sea by a sandbar or similar land features [3]. Also, coastal lagoons are heterogeneous systems formed by different habitats due to their sedimentological, hydrological and biological components [2].

Coastal lagoon ecosystems cover around 13% of the world's coastal areas [3]. About 400 coastal lagoons are covering an area of 640,000 ha in the Mediterranean region. Turkey is the third country among the Mediterranean countries with the most number of lagoons [2].

These ecosystems contribute significantly to groundwater reservoirs, local and regional weather stability, preservation of biodiversity as well as water suppliers both economically and ecologically [1]. The lifespan of lagoons is depended on human-induced structural interventions by changing their morphology [2,3]. Recently, significant environmental

* Corresponding author.

Presented at the 2nd International Conference on Water Problems in the Mediterranean Countries (WPMC-2019), 6–10 May 2019, Nicosia, North Cyprus

concerns about ecological degradation of these sensitive coastal ecosystems have emerged such as pollution and the lack of management [2,4]. Their future is endangered by the misuse of these coastal environments, several pressures they face and their extreme sensitivity to them [5]. Therefore, considering their socioeconomic and environmental value, appropriate management and monitoring of these natural systems are needed [3].

Remote sensing images assist the improvement of resource management strategies as a tool for mapping, monitoring, detecting and evaluating the change in ecosystems. Temporal and spatial analysis of the areas can be performed at global, regional and local levels using a single sensor series or using different satellite data [6–8]. Acquiring multi-date images has become cost-effective with the availability of remote sensing satellites such as Landsat [6] or Sentinel series. Also, it is well known that the combined use of satellite data with different optical wavelengths ensures opportunities for cloudless surface observation [9]. It is an inevitable fact that the new generation Landsat-8 Operational Land Imager (OLI) and Sentinel-2 Multi-Spectral Instrument (MSI) satellite datasets will provide more opportunities in different ecosystem observations at a medium resolution [9,10] such as coastal lagoons. Numerous studies have been conducted for the continuity and combined use of Landsat-8 OLI and Sentinel-2 MSI data on several research topics. For example, Lefebvre et al. [11] successfully combined Sentinel-2 and Landsat-8 images for monitoring urban areas in their study. Van der Werff and Van der Meer [12] aimed to assess the mapping alteration mineralogy results of the Sentinel-2A MSI and compare it with Landsat-8 OLI imagery using band ratio. They found correlation values around 0.8 and higher and also stated that Sentinel-2A MSI can ensure data in case of continuity for Landsat-8 in mineralogy studies. In another research conducted by Lessio et al. [13], the consistency of the combined use of Sentinel-2 and Landsat-8 spectral indices for effective monitoring of crops was tested. They found that the normalized difference vegetation index (NDVI) and normalized difference water index (NDWI) were generally consistent for agricultural studies.

Several image processing algorithms have been proposed to map water bodies such as on-screen digitizing, single-band thresholding [14], multi-band thresholding [15] or classification methods [13,14]. On-screen digitizing requires excessive effort although it is significantly accurate [16]. Another approach is single band thresholding that reveals water information from a multispectral image band via specifying the threshold [15,16]. Also, statistical pattern recognition techniques are used for classification [17]. However, the frequently used method in the extraction of water bodies is multi-band thresholding (i.e. spectral water indices) due to its simplicity. These methods extract water bodies based on the reflectivity differences of each involved band characteristics. The important issue in the extraction of the water body from the indices is the determination of the threshold value that is crucial for distinguishing water bodies from other land cover features. Sezgin and Sankur [18] examined several thresholding approaches and their research qualified Otsu's approach [19], which has been used successfully for different aims in numerous studies such as separation of water bodies and background features [20,21] or built-up and non-built-up land features [22], as the most referenced thresholding method.

There are several studies conducted for a water body and coastal lagoon mapping. For instance, Frihy et al. [23] analyzed the shoreline changes of Manzala Lagoon in Egypt using topographic maps and Landsat series images with unsupervised classification techniques. Frazier and Page [24] delineated water bodies using single-band thresholding and maximum likelihood classification (MLC) techniques from Landsat Thematic Mapper (TM) satellite images in their research. Also, they indicated that Landsat TM images can be used to map water bodies. In another study, Zhang et al. [25] examined Landsat TM and Enhanced Thematic Mapper plus (ETM+) satellite imagery in Ebinur Lake, China with eleven different water extraction algorithms, including the NDWI, modified normalized difference water index (MNDWI), automated water extraction index for shadow ($AWEI_{sh}$) and non-shadow ($AWEI_{nsh}$). Their study resulted in the great potential of Landsat TM and ETM+ images for observing temporal changes in the study area. Similarly, Acharya et al., [16] test the performances of the five different water indices in Nepal (NDVI, NDWI, MNDWI, $AWEI_{sh}$, and $AWEI_{nsh}$) derived from Landsat-8. They pointed out that NDVI and NDWI showed better results. As a result of the comparison of the water indices derived from Landsat ETM+, Landsat-8 OLI and Sentinel-2 MSI in Poyang Lake Basin, China, Zhou et al. [26] determined NDWI as the best indices based on both visual and statistical results with kappa coefficients ranging from 0.77 to 0.92. Additionally, as a result of sensor comparison processes, Landsat-8 and Sentinel-2 reached higher overall accuracy (OA) than that of Landsat ETM+.

Although there are several studies conducted about water body extraction, coastal lagoon monitoring and mapping potential of Landsat-8 and Sentinel-2 images have not been tested yet. Therefore, the objectives of this research are twofold; first, we would like to explore the lagoon mapping potential of Landsat-8 and Sentinel-2 satellite images, and second, we would like to investigate the monitoring potential of Landsat-8 and Sentinel-2 regarding both its continuity and combined use for lagoon monitoring. To achieve these objectives, the spectral consistency of Landsat-8 OLI and Sentinel-2A MSI for coastal lagoon monitoring was investigated using five widely used indices by calculating the correlation coefficient in the first step. Then to achieve the second objective, binary images were created using Otsu's thresholding method [19] and classification algorithm were applied. Moreover, kappa statistics and overall accuracies were calculated to analyze coastal lagoon mapping ability.

2. Materials and methodology

2.1. Study Area

Enez Dalyan Lagoon is located on the shores of the Meriç River Delta, which forms the Turkey-Greece border. Meriç Delta is a transboundary wetland and it is listed as one of the Nationally Important Wetlands of Turkey (Fig. 1).

Dalyan Lake covers an area of approximately 4 km^2 but its' coverage varies based on the amount of the inflows and precipitation. The Lake consists of salty and semi-salty water, and it provides a natural habitat to be nested by

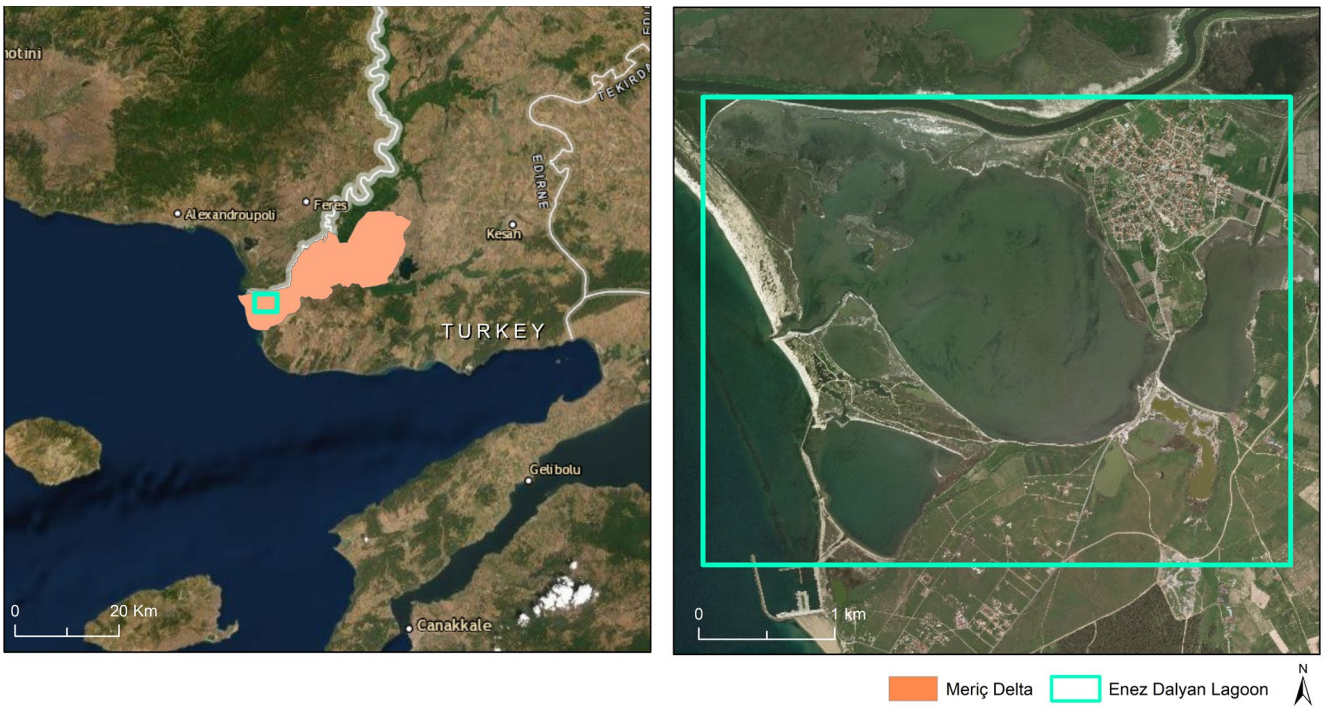

Fig. 1. Location of the study area.

many bird species, especially flamingos. It is in the semi-arid Mediterranean climate zone with cool winters and hot and dry summers. In 1992, Enez coastal lagoons were taken under protection as 2nd-degree Natural Protected Area. Fisheries, animal husbandry and agriculture have an important place in the economy of the district.

2.2. Materials

The main input data of this study is 2018-06-08 dated Landsat-8 OLI and 2018-06-12 dated Sentinel-2 MSI remotely sensed images downloaded from the United States Geological Survey (USGS) Earth Explorer website. The selection of the input images was performed by ensuring maximum closeness in capturing dates as well as the minimum cloud coverage. The Landsat-8 includes eleven bands and equipped with an OLI and Thermal Infrared Sensor (TIRS). TIRS acquires data for the two thermal wavelength regions with a 100 m resolution while OLI obtains data for the visible, near-infrared (NIR) and short-wave infrared (SWIR) with a 30 m resolution and panchromatic wavelength regions with 15 m resolution. On the other hand, the Sentinel-2 which is equipped with the MSI acquires data in thirteen bands involving the visible, NIR, and SWIR wavelength regions with different resolutions ranging from 10 to 60 m. Six bands with similar characteristics were used in this research and specifications of these bands are presented in Table 1.

Also to main input data, Satellite Pour l'Observation de la Terre (SPOT)-7 high-resolution image was used for the validation of the results. 2018-08-03 dated SPOT-7 image was provided by the Istanbul Technical University Application and Research Center for Satellite Communications and Remote Sensing (ITU-CSCRS). SPOT-7 has red, green, blue

Table 1
Band characteristics of Landsat-8 and Sentinel-2 images

	Landsat-8			Sentinel-2		
	Band number	Wavelength (μm)	Spatial resolution (m)	Band number	Wavelength (μm)	Spatial resolution (m)
Blue	2	0.43–0.51	30	2	0.46–0.52	10
Green	3	0.53–0.59	30	3	0.55–0.58	10
Red	4	0.64–0.67	30	4	0.64–0.67	10
NIR	5	0.85–0.88	30	8	0.78–0.90	10
SWIR-1	6	1.57–1.65	30	11	1.57–1.65	20
SWIR-2	7	2.11–2.29	30	12	2.10–2.28	20

and NIR bands with 6 m spatial resolution and panchromatic band with 1.5 m spatial resolution.

2.3. Methodology

This study was composed of four main stages as presented in Fig. 2. Image preprocessing that includes atmospheric correction and geo-shifting was the first stage of the study workflow. Since spatial resolutions of Landsat-8 and Sentinel-2 are different, corresponding bands of Sentinel-2 were resampled to 30 m before processing the data. Landsat image was geographically shifted 5 m to north (y-direction) and west (x-direction) to eliminate the offset errors caused by the images' misalignment [27] using ArcGIS software.

As the second stage of the study, the coastal lagoon was extracted from the input data by applying selected index algorithms and the MLC method, which were explained in detail in the following sections, to both input data.

Investigation of the mapping potential of the applied methodologies and input data was performed in the third stage of the study by explicating the accuracy assessment results. For this purpose, binary images were created using Otsu's thresholding method [19]. The threshold is a dynamic value that varies depending on the sub-pixel land-cover components. Hence, Otsu's thresholding method [19] was applied for the determination of water pixels from index images using ArcGIS software.

Monitoring ability was evaluated in the fourth and the final stage of the study based on the cross-calibration analysis performed between Landsat-8 and Sentinel-2 for each index pair obtained from Landsat-8 and Sentinel-2 datasets. In this context, the Pearson correlation coefficients were determined and scatterplots representing the correlation between each index pair were produced using the R statistical program.

2.3.1. Water indices

Five most commonly used index algorithms of the literature were selected (Table 2) and derived from Landsat-8 and Sentinel-2 images. Tasseled cap wetness index (TCWI) was presented by Crist [28] with experimentally determined coefficients which transformed training pixels into new dimensions with a maximum variability. Since TCWI was designed for TM datasets, empirically determined coefficients may vary for different researches. The coefficients used in this study were determined regarding the existing literature [26].

NDWI was developed by McFeeters [29]. The main aim of this index is to determine open water features using the green (band 2) and NIR (band 4) of Landsat TM. This index minimizes the reflectance of non-water features by using the NIR band while maximizes the reflectance of water by using the green band. Water features have positive values while vegetation of soil has zero or negative values [29]. Another index developed by Xu [15] is MNDWI. Xu [15] stated that water features are mixed with built-up land features with NDWI since they cannot adequately suppress the signal from built-up land. Thus, Xu [15] improved NDWI by replacing the NIR band by mid-infrared band. It is also indicated that this modification can significantly improve the enhancement of water bodies. The last index used in this study was AWEI that was introduced by Feyisa et al., [30] for improving water extraction accuracy with a stable threshold value. This index included two indices which are $AWEI_{sh}$ and $AWEI_{nsh}$. $AWEI_{nsh}$ was developed for urban background areas while $AWEI_{sh}$ was designed to remove shadow pixels. These indices are a linear combination of the blue (band 1), green (band 2), NIR (band 4), SWIR 1 (band 5) and SWIR 2 (band 6) of Landsat TM.

2.3.2. Classification

One of the important parts of the fields of remote sensing, image analysis, and pattern recognition is image classification. A commonly used analytical tool extracting quantitative information from the remotely sensed image is supervised classification. The accuracy of the supervised classification process depends on the number of classes, the accuracy

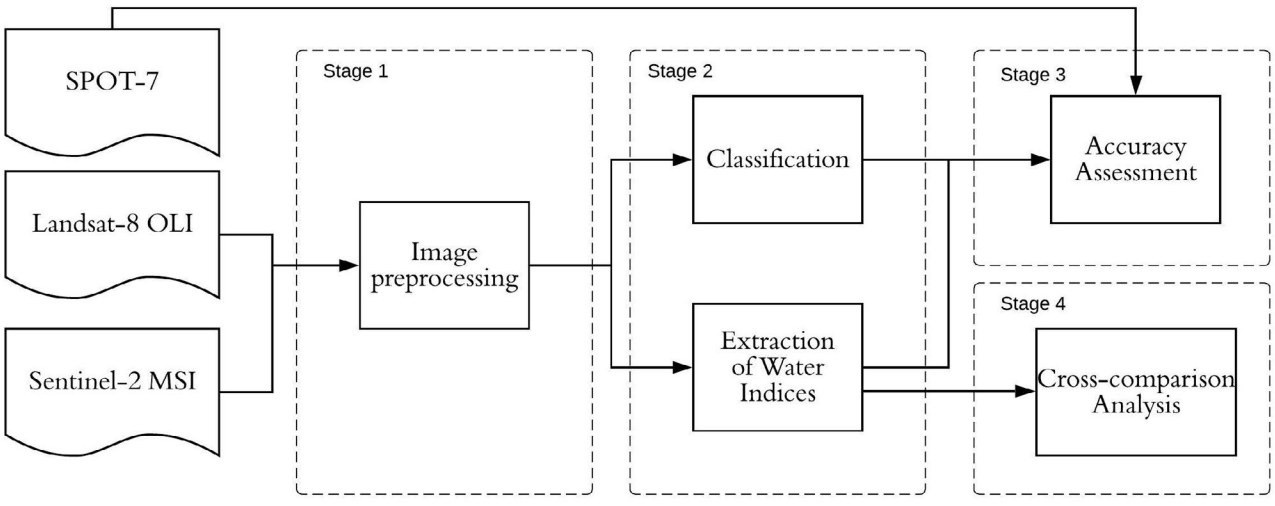

Fig. 2. Flowchart of the study.

Table 2
Selected water indices for the analysis

Index name	Abbreviation	Formulation
Tasseled cap wetness index	TCWI	$0.1509\times\text{Blue}+0.1973\times\text{Green}+0.3279\times\text{Red}+0.3406\times\text{NIR}-0.7112\times\text{SWIR1}-0.4572\times\text{SWIR2}$
Normalized difference water index	NDWI	$\frac{\text{Green}-\text{NIR}}{\text{Green}+\text{NIR}}$
Modified normalized difference water index	MNDWI	$\frac{\text{Green}-\text{SWIR1}}{\text{Green}+\text{SWIR1}}$
Automated water extraction index	AWEI_{sh}	$\text{Blue}+2.5\times\text{Green}-1.5\times(\text{NIR}+\text{SWIR1})-0.25\times\text{SWIR2}$
	AWEI_{nsh}	$4\times(\text{Green}-\text{SWIR1})-(0.25\times\text{NIR}+2.75\times\text{SWIR2})$

of the representation of the statistical characteristics, and the accuracy of the assumptions based on the classification technique. MLC technique, which is one of the widely used supervised classification methods, was selected to be applied in this study. Classification processes completed in ArcGIS software by considering the use of the same training samples for both satellite images.

2.3.3. Accuracy assessment

Accuracy indicates the correctness of the thematic maps which means how thematic maps describe the real land cover type on the ground. Generally, error matrix analysis is widely preferred for accuracy assessment. Although there are several quality measures, OA and Cohen's Kappa statistics (κ) are the common ones. In this study, error matrices were constructed and these quality measures were preferred for the evaluation of accuracy. 100 random points were generated with stratified random sampling method was used for the collection of the reference data. The accuracy of the water body mapping results from the different methods and sensors were evaluated to the very high-resolution SPOT-7 imagery.

3. Results

3.1. Coastal lagoon extraction

TCWI, NDWI, MNDWI, AWEI_{sh}, and AWEI_{nsh} were derived from Landsat-8 and Sentinel-2 satellite images for all datasets and thematic maps were produced using Otsu's thresholding method [19]. Furthermore, the classification map was produced via a classification algorithm. As seen in Fig. 3, the channel that came from the Meriç River and connected to the right part of the lake was best seen in the images derived from AWEI_{nsh}. Although this channel was found in AWEI_{sh}-derived images, this index produced more noisy results visually. Although this lagoon was extracted better with AWEI_{nsh}, the small island in the middle of the lagoon could not be determined by these indices. TCWI gave the worst result irrespective of the sensor. The right part of the lake cannot be determined correctly with NDWI.

In general, although Landsat-8 and Sentinel-2 yield very close visual and statistical results, Sentinel-2 produced more noisy results than Landsat-8. MLC has completely extracted the island in the middle of the lake. However it did not produce results as good as AWEI_{nsh} in the determination of the shorelines.

3.2. Coastal lagoon mapping potential

According to the statistical results presented in Table 3, AWEI_{nsh} derived from Landsat-8 and Sentinel-2 had the highest Kappa (0.84) and OA (92%) values which are consistent with visual interpretation. After that, MLC and MNDWI (with κ:0.82 and OA:91%) derived from Sentinel-2 and NDWI (with κ:0.80 and OA:90%) derived from Sentinel-2 reached the highest statistical results, respectively. Generally, except for MLC derived from Landsat-8, very high statistical results were achieved. MLC derived from Landsat-8 had the lowest Kappa (0.70) and OA (83%) values.

When the areal results were taken into consideration (Table 4), the minimum difference was obtained with AWEI_{nsh} derived from Landsat-8 and Sentinel-2 images with 14.58 hectares, while the highest difference was obtained from the classification algorithm. It can be said that the AWEI_{nsh} results derived from Landsat-8 and Sentinel-2 gave very similar results.

3.3. Coastal lagoon monitoring potential

In this study, correlations between Landsat-8 OLI and Sentinel-2 were evaluated by computing Pearson's correlation coefficients. The correlation coefficients were calculated for each pair of the index algorithms, which derived from Landsat-8 and Sentinel-2 satellite images. Scatterplots of the cross-comparison results presented in Fig. 4. In Fig. 4, the *x* and *y*-axis depicted Landsat-8 and Sentinel-2 data respectively. Based on the scatterplots, AWEI_{nsh} had the highest correlation value with 0.989, while NDWI had the lowest correlation value with 0.966. However, it should be emphasized that all indices for this test area had a quite high correlation value and Sentinel-2 and Landsat-8 had similar results. Cross-comparison results outlined a good agreement between almost all datasets.

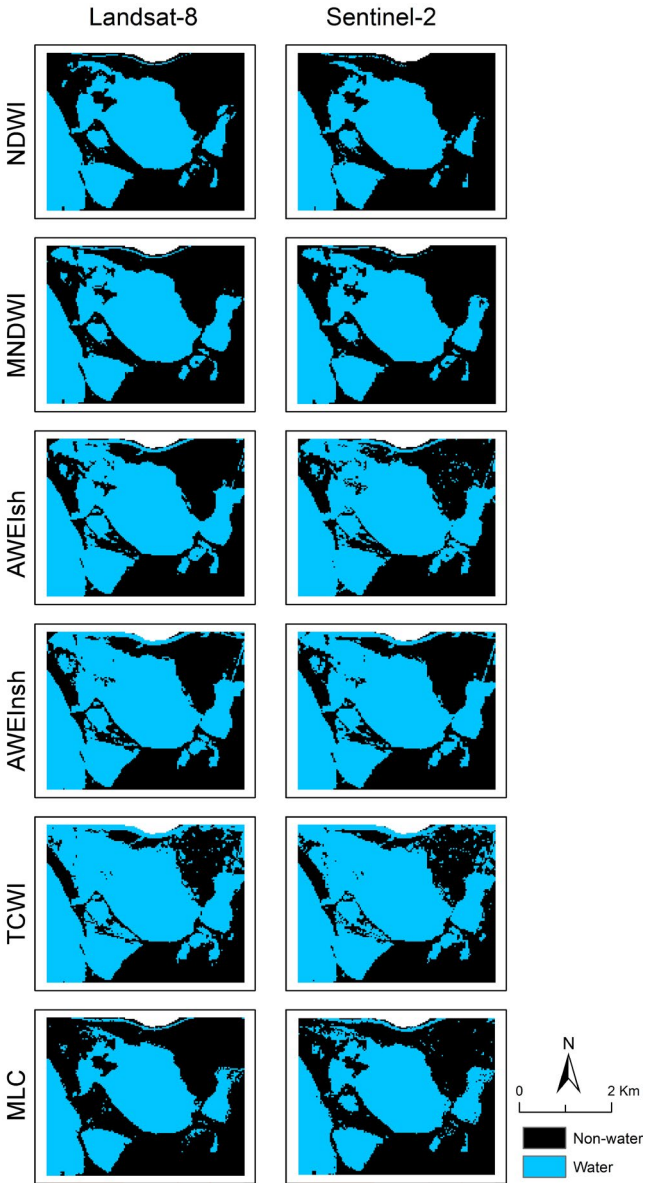

Fig. 3. Waterbody mapping results of different image processing algorithms in Enez Dalyan Lagoon.

Table 3
Statistical results of the mapping algorithms

	Kappa		OA (%)	
	Landsat-8	Sentinel-2	Landsat-8	Sentinel-2
NDWI	0.76	0.80	88.00	90.00
MNDWI	0.78	0.82	89.00	91.00
$AWEI_{sh}$	0.78	0.78	89.00	89.00
$AWEI_{nsh}$	**0.84**	**0.84**	**92.00**	**92.00**
TCWI	0.76	0.78	88.00	89.00
MLC	0.70	0.82	83.00	91.00

Table 4
Areal results of the mapping algorithms in hectares

	Landsat-8		Sentinel-2	
	Water	Non-water	Water	Non-water
NDWI	655.47	820.62	632.79	843.3
MNDWI	719.28	756.81	690.93	785.16
$AWEI_{sh}$	807.57	668.52	834.93	641.16
$AWEI_{nsh}$	850.59	625.5	836.01	640.08
TCWI	934.56	541.53	918.09	558.00
MLC	621.81	854.28	679.23	796.86

4. Discussion and conclusion

This study aimed to investigate the coastal lagoon monitoring and mapping potential of Landsat-8 OLI and Sentinel-2 satellite images. Although Landsat-8 OLI and Sentinel-2 MSI have similar characteristics, assessment is recommended since some band combinations vary in different sensors [12,31]. There have been various studies investigated the continuity and combined use of Landsat-8 OLI and Sentinel-2 MSI data on numerous research topics such as urban studies [11], mineralogy mapping [12] and agricultural studies [13]. In this study, correlation coefficients between 0.966 and 0.989 were obtained in good agreement with the research presented by Mandanici [31] who obtained correlation coefficients of NDWI varying from 0.78 to 0.99 for different test areas.

Among the methods, the $AWEI_{nsh}$ achieved quite better results compared with the other methods for the mapping of Enez Dalyan Lagoon while TCWI had relatively poor results independent from the sensors. Index algorithms, which are fast and accurate than conventional classification methods provide a mapping of Enez Dalyan Lagoon.

Remote sensing technology provides fast and easy coastal lagoon mapping over time which is useful in areas such as the selected research area Furthermore, Landsat-8 OLI and Sentinel-2 MSI sensors which are statistically consistent provide monitoring of Enez Dalyan Lagoon regarding both continuity and combined use. These extremely fragile and both socio-economically and environmentally important coastal ecosystems are being misused due to lack of management. The combined use of these two satellite images increases temporal resolution significantly and therefore is very favorable in mapping and monitoring of coastal lagoons for proper management. With the opportunities provided by remote sensing technology, it can produce meaningful, fast and high-quality results as in many sectors and produce effective input data in studies such as water management.

Acknowledgments

We would like to thank Istanbul Technical University Application and Research Center for Satellite Communications and Remote Sensing (ITU-CSCRS) for providing the SPOT-7 data set.

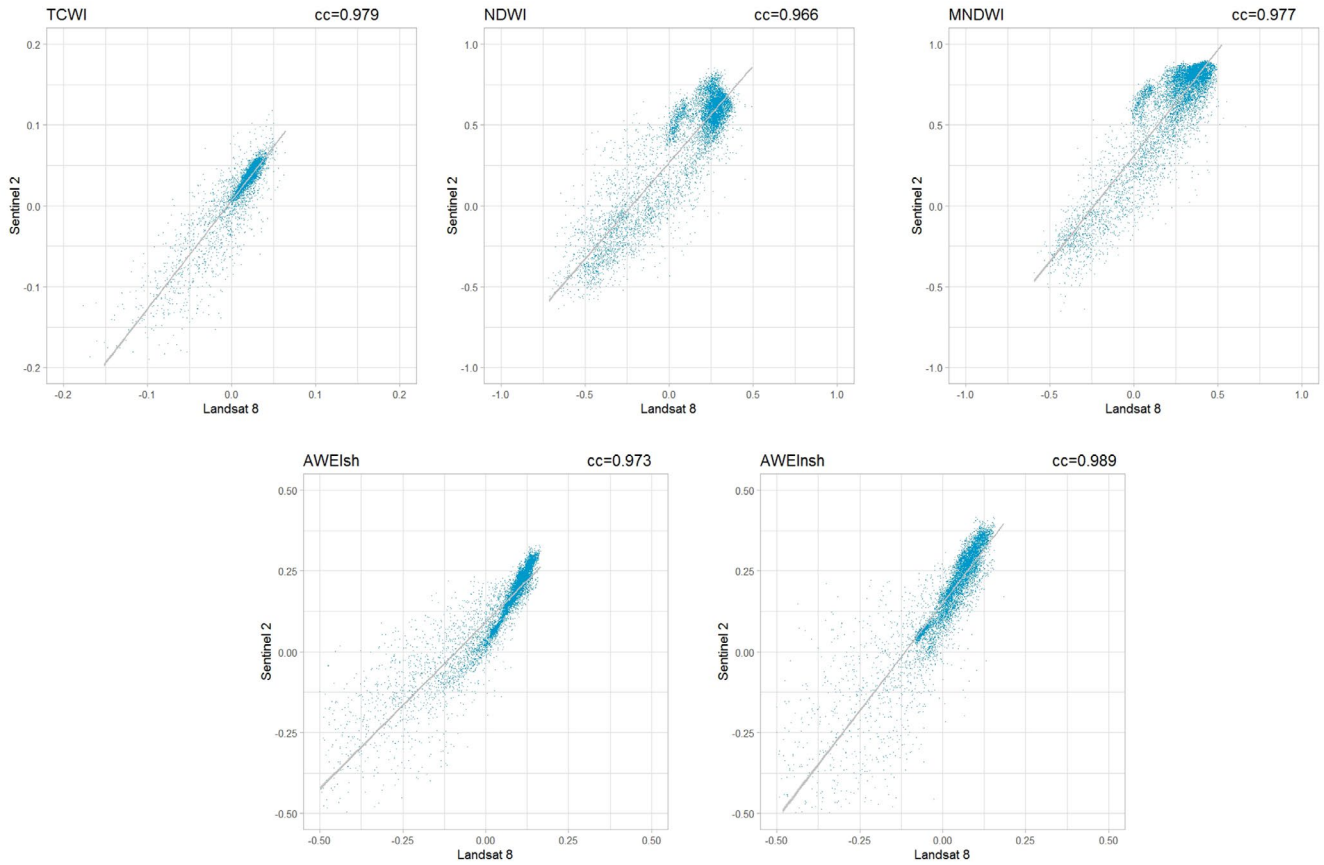

Fig. 4. Scatterplots that shows the cross-comparison results. 'cc' stands for the correlation coefficient.

References

[1] M.C. Hennemann, M.M. Petrucio, Spatial and temporal dynamic of trophic relevant parameters in a subtropical coastal lagoon in Brazil, Environ. Monit. Assess., 181 (2011) 347–361.

[2] S. Cataudella, D. Crosetti, F. Massa, Eds., Mediterranean Coastal Lagoons: Sustainable Management and Interactions Among Aquaculture, Capture Fisheries and the Environment. Studies and Reviews, General Fisheries Commission for the Mediterranean 95, Food and Agriculture Organization of the United Nations, Rome, 2015.

[3] A. Pérez-ruzafa, I.M. Pérez-ruzafa, A. Newton, C. Marcos, Coastal Lagoons: Environmental Variability, Ecosystem Complexity, and Goods and Services Uniformity, Coasts and Estuaries, Elsevier Inc., New York, 2019, pp. 253–276.

[4] M. Necibi, N. Mzoughi, M.N. Daly Yahia, O. Pringault, Distributions of organochlorine pesticides and polychlorinated biphenyl in surface water from Bizerte Lagoon, Tunisia, Desal. Wat. Treat., 56 (2015) 2663–2671.

[5] H. Alphan, T.K. Yilmaz, Monitoring environmental changes in the Mediterranean coastal landscape: the case of Cukurova, Turkey, Environ. Manage., 35 (2005) 607–619.

[6] M.H. Ahmed, B.M. El Leithy, J.R. Thompson, R.J. Flower, M. Ramdani, F. Ayache, S.M. Hassan, Application of remote sensing to site characterisation and environmental change analysis of North African coastal lagoons, Hydrobiologia, 622 (2009) 147–171.

[7] V. Markogianni, E. Dimitriou, Landuse and NDVI change analysis of Sperchios river basin (Greece) with different spatial resolution sensor data by Landsat/MSS/TM and OLI, Desal. Wat. Treat., 57 (2016) 29092–29103.

[8] S.J. Ki, D.J. Jeon, J.H. Kim, Influence of spatial resolution of radar images on the parameterization and performance of SWAT model, Desal. Wat. Treat., 57 (2016) 27548–27556.

[9] J. Li, D.P. Roy, A global analysis of Sentinel-2A, Sentinel-2B and Landsat-8 data revisit intervals and implications for terrestrial monitoring, Remote Sens., 9 (2017) 902.

[10] D.P. Roy, M.A. Wulder, T.R. Loveland, C.E. Woodcock, R.G. Allen, M.C. Anderson, D. Helder, J.R. Irons, D.M. Johnson, R. Kennedy, T.A. Scambos, C.B. Schaaf, J.R. Schott, Y. Sheng, E.F. Vermote, A.S. Belward, R. Bindschadler, W.B. Cohen, Z. Zhu, Landsat-8: science and product vision for terrestrial global change research, Remote Sens. Environ., 145 (2014) 154–172.

[11] A. Lefebvre, C. Sannier, T. Corpetti, Monitoring urban areas with Sentinel-2A data: application to the update of the Copernicus high resolution layer imperviousness degree, Remote Sens., 8 (2016) 606.

[12] H. van der Werff, F. van der Meer, Sentinel-2A MSI and Landsat 8 OLI provide data continuity for geological remote sensing, Remote Sens., 8 (2016) 11.

[13] A. Lessio, V. Fissore, E. Borgogno-Mondino, Preliminary tests and results concerning integration of Sentinel-2 and Landsat-8 OLI for crop monitoring, J. Imaging, 3 (2017) 9.

[14] S.K. Jain, R.D. Singh, M.K. Jain, A.K. Lohani, Delineation of flood-prone areas using remote sensing techniques, Water Resour. Manage., 19 (2005) 333–347.

[15] H.Q. Xu, Modification of normalised difference water index (NDWI) to enhance open water features in remotely sensed imagery, Int. J. Remote Sens., 27 (2006) 3025–3033.

[16] T.D. Acharya, A. Subedi, D.H. Lee, Evaluation of water indices for surface water extraction in a Landsat 8 scene of Nepal, Sensors (Switzerland), 18 (2018) 1–15.

[17] L.Y. Ji, X.R. Geng, K. Sun, Y.C. Zhao, P. Gong, Target detection method for water mapping using Landsat 8 OLI/TIRS imagery, Water (Switzerland), 7 (2015) 794–817.

[18] M. Sezgin, B. Sankur, Survey over image thresholding techniques and quantitative performance evaluation, J. Electron. Imaging, 13 (2004) 146–165.

[19] N.Y. Otsu, A threshold selection method from gray-level histograms, IEEE Trans. Syst. Man Cybern., 9 (1979) 62–66.
[20] Z.Q. Du, W.B. Li, D.B. Zhou, L.Q. Tian, F. Ling, H.L. Wang, Y.M. Gui, B. Sun, Analysis of Landsat-8 OLI imagery for land surface water mapping, Remote Sens. Lett., 5 (2014) 672–681.
[21] Y.H. Ren, Y. Liu, Surface water classification from GF-4 images using a time series water index, Int. J. Remote Sens., 40 (2019) 6336–6364.
[22] K. Ezimand, A.A. Kakroodi, M. Kiavarz, The development of spectral indices for detecting built-up land areas and their relationship with land-surface temperature, Int. J. Remote Sens., 39 (2018) 8428–8449.
[23] O.E. Frihy, Kh.M. Dewidar, S.M. Nasr, M.M. El Raey, Change detection of the northeastern Nile Delta of Egypt: shoreline changes, Spit evolution, margin changes of Manzala lagoon and its islands, Int. J. Remote Sens., 19 (1998) 1901–1912.
[24] P.S. Frazier, K.J. Page, Water body detection and delineation with Landsat TM data, Photogramm. Eng. Remote Sens., 66 (2000) 1461–1467.
[25] F. Zhang, T. Tiyip, H.-T. Kung, V.C. Johnson, J. Wang, I. Nurmemet, Improved water extraction using Landsat TM/ETM+ images in Ebinur Lake, Xinjiang, China, Remote Sens. Appl.: Soc. Environ., 4 (2016) 109–118.
[26] Y. Zhou, J.W. Dong, X.M. Xiao, T. Xiao, Z.Q. Yang, G.S. Zhao, Z.H. Zou, Y.W. Qin, Open surface water mapping algorithms: a comparison of water-related spectral indices and sensors, Water (Switzerland), 9 (2017) 4.
[27] M. Arekhi, C. Goksel, F. Balik Sanli, G. Senel, Comparative evaluation of the spectral and spatial consistency of Sentinel-2 and Landsat-8 OLI data for Igneada Longos Forest, ISPRS Int. J. Geo-Inf., 8 (2019) 56.
[28] E.P. Crist, A TM tasseled cap equivalent transformation for reflectance factor data, Remote Sens. Environ., 17 (1985) 301–306.
[29] S.K. McFeeters, The use of the Normalized Difference Water Index (NDWI) in the delineation of open water features, Int. J. Remote Sens., 17 (1996) 1425–1432.
[30] G.L. Feyisa, H. Meilby, R. Fensholt, S.R. Proud, Automated Water Extraction Index: a new technique for surface water mapping using Landsat imagery, Remote Sens. Environ., 140 (2014) 23–35.
[31] E. Mandanici, G. Bitelli, Preliminary comparison of Sentinel-2 and Landsat 8 imagery for a combined use, Remote Sens., 8 (2016) 12.